

## Quality assessment of ZnO-based varistors by 1/f noise

Lech Z. Hasse<sup>1</sup>, Sylwia Babicz<sup>1</sup>, Leszek Kaczmarek<sup>1</sup>, Janusz M. Smulko<sup>1</sup>, Vlasta Sedlakova<sup>2</sup>

<sup>1</sup> Gdansk University of Technology, Gdansk, Poland

<sup>2</sup> Brno University of Technology, Brno, Czech Republic

### Abstract

Noise has been used as a diagnostic tool of surge arrester varistor structures comprising of ZnO grains of various type and size. The physical and electrical properties of the measured samples have been described. In the experimental study, the applied measurement system and the results of noise measurements for the selected structures of varistors designed for the continuous working voltage 280 V, 440 V and 660 V have been presented. Noise properties are related to electrical characteristics of the measured specimens giving more distinctive results than their voltage-current characteristics. It is suggested that the proposed procedure can be applied as an effective non-destructive testing method focused on defects and structural heterogeneity detection in the tested objects to assess their preparation processes.

**Keywords:** ZnO varistor, low-frequency noise, diagnostics, reliability

### 1. Introduction

Measurements of noise are a promising method for non-destructive quality assessment of the tested objects, like passive electronic elements, semiconductor devices or corrosive objects [1–3]. Most of the failures result from various defects and imperfections created during the manufacture processes. The excessive 1/f noise component is very sensitive to any defects in the tested structures and this is the main reason why the 1/f noise is efficient tool for quality prediction.

The investigated ZnO-based (further also shortly: ZnO) varistor structures comprise of ZnO grains of different physical properties which determine their non-linear terminal voltage-current characteristics. We can expect that the grains of different potential barriers exhibit various 1/f noise intensities which can be used for their quality prediction. Thus, we prepared two batches of the specimens of two different qualities (poor and high) and selected by experimental investigation of their bias conditions (DC current-voltage characteristics). First, we present electrical properties of the tested structures and enclose their preparation processes. Next, we describe the applied noise measurement setup and compare the estimated 1/f noise spectra with other parameters of their electrical properties to confirm that noise measurements are very effective for characterization of the grained ZnO structures. Now, we present a more in-depth analysis of noise observed in ZnO structures and consider efficiency of the new method of varistors quality assessment when compared with earlier published results of Third Harmonic Index (THI), Resonant Ultrasound Spectroscopy (RUS), Electro-Ultrasonic Spectroscopy (EUS) and preliminary low-frequency noise measurements [4-7]. Varistor quality evaluation can be realized also using variable-temperature dielectric spectroscopy [8] or more generally, impedance spectroscopy [9]. We have also used impedance spectroscopy as a tool for

a varistor quality evaluation [6] applying a special measurement probe for high impedance spectroscopy [10]. 1/f noise phenomena and conducting mechanisms were intensively studied also in grainy polymer [11] and composite [12] thick-film layers in wide temperature range [13].

### 1.1. Structures of ZnO grains

Polycrystalline semiconducting ceramics of ZnO grains are used in overvoltage protecting devices due to their nonlinear current-voltage characteristics. The cylindrically-shaped ZnO structures are typically used for various high-voltage ranges. Their properties depend on technological conditions at different production stages of their shape forming and firing (how the applied materials are milled, mixed and squeezed). The applied ceramics comprises of ZnO and some additives (oxides of bismuth, cobalt, manganese) which considerably influence their electrical properties. Molar composition of varistor can range from 85 to 98% ZnO and the rest of other oxides. The bulk ceramic contains predominately grain-boundary barrier junctions. The Schottky barriers reveal a breakdown voltage of about 3 V per inter-granular barrier. The microstructure uniformity and defects directly decide about the performance of these multi-junction devices. Dopant effects on grain boundary barriers, sintering behavior and microstructure [14]. The oxide mixing process for homogeneity is executed in high sintering temperatures (up to about 1300 °C) to achieve a proper density. Consequently, microstructural heterogeneity, large average grain sizes (typically 10-20 μm in diameter) and also high porosity caused by exaggerated grain growth in high-temperature sintering, determine the limited performance of ZnO-based varistors. The grains differ in geometry but are very similar with respect to chemical composition. The grain size can be controlled by sintering temperature and time and also by different additives. Higher sintering temperature and longer sintering times increase the grain size [16]. The grain boundaries have been found to give rise to the nonlinear I-V characteristics by formation of barriers against electrical conduction.

Popular low-voltage varistors can be prepared by multilayer technology [17] or low temperature co-fired ceramics technology [18].

The ZnO structures have a strongly non-ohmic current-voltage characteristic and therefore are used to protect electrical circuits and networks against excessive voltage transients shunting the current created by this voltage away from the sensitive elements. All varistors are tested at final stage of their production by a leakage current measurement at relatively low voltage or by determining their ability to sustain intense current flows at a given interval of tens of μs. The mentioned tests can be destructive or are not too sensitive to some tiny changes of technology at their production. Therefore, the new nondestructive measurement methods are desired.

### 1.2. Varistors electrical properties

The current-voltage characteristics of a varistor applied in a surge arrester has three distinguishable regions: pre-breakdown, breakdown or leakage area and saturation (high-current) (Fig. 1). A varistor behaves as a highly resistive resistor ( $\sim 10^9 \Omega$ ) at low voltage region. At leakage (breakdown) region varistors have peculiar, highly nonlinear properties described by the empirical equation between current  $I$  and the applied voltage  $U$ :

$$I = k \cdot U^\alpha \quad (1)$$

where  $k$  is a constant and  $\alpha$  is a non-ohmic parameter indicating the resistivity of the varistor changing nonlinearly with the voltage. The parameter  $\alpha$  depends on a type of boundary junctions which exist between the grains and can be 60 or higher in this area. Varistors saturate at higher voltages and when the voltage reaches this level the resistance of a varistor drops rapidly and does not exceed tens of ohms. For very large currents a conductance of a varistor will be limited by the internal conductance of the ZnO grains. They should exhibit as much as possible nonlinear characteristics (it means high value of a parameter  $\alpha$ ). The macroscopic properties of a varistor are determined by the structural and chemical properties of the microscopic level. There are good, low nonlinear and linear junctions between the ZnO grains. The exponent  $\alpha > 30$  indicates the most required highly nonlinear grain contacts. The low nonlinear contacts exhibit typically  $\alpha \approx 10$ . These various contacts can be discriminated by a shape of their current-voltage characteristics (Fig. 1).

A real varistor is a mixture of various grains within the ZnO structure and its characteristics depends on the content of the grain types in their structure. The widespread presence of linear or weakly nonlinear grain contacts decreases  $\alpha$  and diminishes a desirable nonlinear varistor characteristic at its relatively low voltage region. This fact provides a significant number of poor quality ZnO structures. The ZnO grains are typically 10÷20  $\mu\text{m}$  in diameter and have very similar chemical composition. The grain size is controlled by temperature and time of sintering but also by a composition of different additives.

The firing is the most important part in the process of varistor production and strongly affecting its electrical properties. Even the same composition of oxides results in different structural phases and electrical characteristics depending on different sintering conditions (temperature and atmosphere) [16]. The current-voltage characteristics is controlled by the electrostatic barriers at the interfaces between grains originating from interface charge stemming from lattice mismatch, defects and dopants at the grain boundary. The interface charge changes the Fermi level in the vicinity of the grain boundary. A different grain size, which is connected with slightly different chemical structure, results in different mechanisms of current conductivity. A barrier height depends on a grain size and directly on the deep bulk traps. The barriers fluctuate and this fact influences noise phenomena generated in ZnO structures which result from fluctuations within potential barrier between the grains. We can suppose that these fluctuations can be considered as a more sensitive indicator for a varistor quality assessment. Additionally, we can claim that different grains will affect different humidity absorption within a varistor structure which takes place in practice, at rainy conditions and results in varistor failure due to excessive overheating during overvoltage pulses. Thus, results of noise measurements could inform about varistor current state and its ability of working at harsh humid atmosphere.

## 2. Tested varistors

Three types of varistors having different continuous operating voltages (280 V, 440 V and 660 V - hereinafter referred to as 280, 440 and 660 type, respectively) have been investigated. All varistors have the same diameter (30 mm) but the higher voltage threshold is obtained for the thicker samples: 2.9 mm (280 type), 4 mm (440 type) and 5.8 mm (660 type) – see Fig. 2.

Two batches of samples (containing 100 specimens each) for the every mentioned above voltage were produced in a big industrial plant for testing purposes. There was a significant difference between constituents of the grains having linear and nonlinear junctions in each group as a result of artificially and intentionally introduced changes at their technology, as happens accidentally at their

production. The changes were a result only of different sintering temperatures for both type of batches. The chemical composition was the same for both batches of samples and was known only for producer as a production reservation for commercially produced surge arresters. The aggregated grains formed a structure which determined the final current-voltage characteristics, having noticeable differences between both groups of varistors. One of the batches could be treated as a group of varistors having poor quality – with a higher leakage current. The grains structure in such a specimen was investigated only by an Atomic Force Microscope (AFM) type N-Tegra Prima of NT-MDT company. We scanned its surface to identify the differences in size of grains between the batches. The system measures an interaction between the probe and the surface of a varistor during its scanning by means of a laser beam. The exemplary images of the scanned surfaces (having dimensions of  $50\ \mu\text{m} \times 55\ \mu\text{m}$ ) are shown in Fig. 3. The well-prepared ZnO structures comprised of relatively big grains having non-linear current-voltage junction characteristics (Fig. 3a). The smaller grains (having often only ohmic contacts) resulted in a more linear current-voltage characteristic (Fig. 3b).

The difference between the batches is more visible when the dimensions of detected grains are compared. The size, diameter and volume were estimated by NOVA software which analyzed pictures taken by the applied AFM. Before the analysis, we detected the edge of grains by the Laplace filter. After filtering, the difference between the batches is clearly noticeable (Fig. 4). We estimated averages of four typical statistics parameters for both of specimens (Tab. 1).

The discrepancy between the topographies of both type of samples is also visible by comparing height histograms of these different samples (Fig. 5). The poor quality specimen has Gaussian distribution of pixel heights (Fig. 5 b) while the well-prepared specimen has more pixels with high and low height without Gaussian distribution (Fig. 5a).

Industrial standards recommend leakage current measurements at a high voltage, e.g. about 400 V for varistors designed for continuous operating voltage 280 V (for varistors of 280 type). An occurrence of higher overvoltages during exploitation causes intense current flows, mainly through the narrow paths created by the grains with linear (ohmic) junctions. High current density and intensive overheating within vicinity of such paths results in irreversible local destruction of ZnO structure.

Significant differences in electrical properties between the specimens of high and poor quality can be observed in current-voltage characteristics (Fig. 6). The samples of poor quality (having smaller grains) saturate at a significantly lower voltage (have higher leakage current at the same bias voltage). Such difference between the samples can be identified as well by measuring nonlinearity of their characteristic. This can be done when the sample is stimulated by harmonic voltage and intensity of the third harmonic component is measured [4]. This method is more difficult in practice in comparison to a leakage current measurement requiring high power voltage supplier and the well-designed filters to attenuate the stimulating harmonic voltage in a detector circuit.

### 3. Noise measurement setup

The block diagram of the noise measurement system is shown in Fig. 7. For high-voltage varistors noise can be observed when the specimen is polarized by the bias voltage higher than 400 V and the current flowing through the sample has sufficiently intense random component to be measured accurately.

The prepared head with five independent contact electrodes at each varistor side was implemented into the system with a low-level noise signal preamplifier having the front-end adopted for high-voltages (Fig. 8). We applied a high-voltage supplier (Glassman EH3R33L) with an RC filter comprising of a few RC sections (R1C1, R2C2, R3C3, R4C4). A voltage  $U$  across the tested varistor was measured by a voltmeter attached to the varistor terminals (Fig. 8) and a DC current  $I$  flowing through the tested sample was controlled by  $U_1$ . For voltages up to about 400÷700 V the DC varistor resistance was no lower than tens of  $G\Omega$ . Only for voltages above these values the DC current flowing through the tested specimen was enough high (more than ten of  $\mu\text{A}$ ) to generate sufficiently intense noise component within the sample which begun to overwhelm the measurement system background noise, sometimes even a few orders of magnitude. These measurement conditions were a compromise: the DC current should be enough high to make a noise level accurately and easily measurable above the background noise and enough low not to heat up excessively a measured sample.

The DC component was blocked by a capacitor C5 and the voltage fluctuations at the output of operational amplifier OPA128 were amplified twice in this step and adjusted finally to the applied spectrum analyzer by the low-noise voltage amplifier Stanford SR560. The specimen was placed in an accurately shielded metal box to reduce outside interferences. The measurement setup was supplied by batteries except the high-voltage DC supplier which was attached to the specimen by previously mentioned RC filters.

#### 4. Experimental results

The preliminary results of noise measurements in the frequency interval up to 6.4 kHz for varistors 280 type biased by the DC current equal to 11  $\mu\text{A}$  are shown in Fig. 9. The background noise level of the measurement system was below  $10^{-26}$  [ $\text{A}^2/\text{Hz}$ ] at 1 kHz and about  $10^{-24}$  [ $\text{A}^2/\text{Hz}$ ] at 10 Hz. Strong spectral lines caused by power line interferences were present even for measurements in a Faraday Cage. The appreciable interference spectral line at  $f = 50$  Hz can be seen in Fig. 9 when the measured varistor was biased. However it did not influence significantly on the noise measurement results. Typically, the  $1/f$  noise was overwhelming in the frequency range up to a few kHz in the tested varistors. At higher frequencies the white noise component dominated.

Very strong differences (even more than 30 dB) between the power spectral densities of current fluctuations  $S_I(f)$  (proportional to the squared varistor DC current  $I$ , see Fig. 10a) observed in different samples responded to visible differences in their DC current-voltage characteristics (Fig. 10b). According to the widely-used and verified Hooge relation [19], the quadratic dependence between a current spectral density  $S_I(f)$  and a current  $I$  enables an evaluation of the bulk noise intensity suggests that the observed noise is generated within the volume of the investigated ZnO structure [20].

Some specimens (e.g. the sample no. 63) exhibited significantly higher leakage currents at relatively low DC voltages. It has been proved by AFM images that the high contents of small grains (assuring almost linear boundary junctions between the grains) occurred in such structures and generated very intense  $1/f$  noise component. Very similar behavior was observed in other materials or structures when changes in current-voltage characteristics influenced a low frequency noise [20, 21].

Another type of varistors having also a strongly nonlinear DC current-voltage characteristics (e.g. sample no. 60) was observed. Such sample was built from the grains having nonlinear contacts as well which resulted in nonlinear characteristics (e.g. the varistor no. 45) but slightly worse than the

best samples (e.g. the sample no. 60). In this case the  $1/f^m$  noise (for  $m \approx 0.4$ ) was comparable with other samples having nonlinear characteristics and low leakage currents which was considerably lower than in the samples with numerous grains having ohmic boundary junctions and more intense leakage current (e.g. the sample no. 63).

It can be noted that the scale in Fig. 10b is lin-log and the relative changes of I-V characteristics between the high and poor quality samples are significantly smaller than for noise (Fig. 10a, scale log-log, differences several orders of magnitude). This is a reason for preferring noise measurements which are even a few orders more sensitive to any changes of varistors technological parameters.

The next exemplary results of noise measurement polarized at much intense DC current  $I = 200 \mu\text{A}$  for another set of varistors are shown in Fig. 11. The poor quality specimens (having smaller grains of more linear characteristic of boundary junctions), designed for three different working voltages (280, 440 and 660 type, respectively), exhibited strongly higher  $1/f$  noise component than the high quality samples (characterized by bigger grains of nonlinear boundary junctions) of the same type. It corresponds to changes of the I-V characteristics especially in the important range of voltages for their exploitation conditions.

## 5. Data analysis and discussion

According to the Hooge model of low frequency fluctuations [19-21], the  $1/f$  noise is no surface effect but fundamentally a bulk phenomenon, where an empirical relation between current power spectral density  $S_I(f)$  and DC polarizing current  $I$  exists:

$$\frac{S_I(f)}{I^2} = \frac{\alpha_H}{N \cdot f} \quad (2)$$

where  $N$  is the total number of atoms in the sample and  $\alpha_H$  known as a Hooge constant – an empirical parameter describing how noisy is the investigated structure.

In a case of ZnO structures having various grain sizes of different boundary junctions we can suppose that mechanisms of conduction and  $1/f$  noise generation can vary due to strong differences between the grains. This problem was investigated more in depth for relatively small ZnO structures working in low-voltage electronic circuits and protecting against overvoltage pulses of amplitude of tens of volts only [22-24] or in microscopic objects (nanoparticle wires) [25] or other grainy resistive structures [26]. The currently investigated specimens had more than ten's times greater volume than the reported in the earlier papers [23, 24] but had a grain size of the same range ( $10 \div 25 \mu\text{m}$ ) as previously investigated due to similar production methods and the applied impurities. Thus, we decided to measure  $1/f$  noise at greater DC current  $I$  to assure similar current density as reported in former experiments [23].

When  $I = 200 \mu\text{A}$  we observed  $1/f$  noise which dominated at low frequency range, at least within the band  $5 \div 1000 \text{ Hz}$  (Fig. 11). The thickness of measured varistor samples 280, 440 and 660 type, was ca. 3 mm, 4 mm and 5 mm, respectively. Therefore the number of noise sources is proportional to the sample thickness and power spectral density  $S_I(f)$  should be inversely proportional to this thickness according to the Hooge model relation (2). In Fig.11 one can see that the relation between  $S_I(f)$  e.g. at 200 Hz is for high quality samples 280 type and 440 type almost exactly equal as





4:3. For the sample 660 type trend is the same, however the noise level is lower due to the small value of current not exciting the all noise sources and not allowing to receive the proper quantitative data.

At lower currents ( $I = 11 \mu\text{A}$ ) some high quality samples exhibited dependence of  $S_I(f)$  on frequency as  $1/f^{0.4}$  (Fig. 9). It suggests that such low bias current is too small to get reliable data at least for some of the investigated samples due to too low noise level and limited sensibility of the measurement setup or instable conduction mechanisms through high potential barriers between the grains.

The hitherto reported investigations on conduction mechanisms and  $1/f$  noise in ZnO varistors confirmed that the main mechanism of  $1/f$  noise is due to mobility fluctuations by considering a series of Schottky barriers which exist between the grains [23]. Moreover, there is additional evidence that in the ohmic region (the pre-breakdown region at Fig. 1), at bias voltage below 100 V, the normalized power spectral density  $S_I(f)/I^2$  depends linearly with DC resistance of the samples prepared in similar way. Then, we can find that for homogenous ZnO samples with neglected contact noise the observed  $1/f$  noise component can be derived by a more specific formula [27, 28]:

$$\frac{S_I(f)}{I^2} = \frac{\alpha_H \mu q R}{L^2 \cdot f} \quad (3)$$

where  $R$  – the resistance between varistor contacts at a distance  $L$ ,  $\mu$  – the mobility and  $q$  – the electron charge. Equation (3) assumes that the number of free carriers is equal  $N = L^2/q\mu R$  in the investigated structures. In fact, the number  $N$  is difficult to be properly estimated in heterogenous samples as the investigated specimens comprise of different grains. Thus, we propose to utilize another way of using power spectral density  $S_I(f)$  analysis to differentiate a quality of ZnO structures by means of low frequency noise.

We propose, as suggested in [27, 28], to consider  $S_I(f)$  as a sum of  $1/f$  noise generated independently in number of grains  $N_g$ :

$$\frac{S_I(f)}{I^2} = N_g^{-1} \frac{S_{I_g}(f)}{I_g^2} \quad (4)$$

where  $S_{I_g}(f)$  represents an averaged current power spectral density of noise generated by fluctuations of the current  $I_g$  flowing between the grains. The value of  $N_g$  can be estimated by means of AFM measurements and grain size distribution, as presented before (Fig. 4 and Fig. 5, Tab. 1). Then, we have two different factors:  $S_I(f)$  and  $S_{I_g}(f)$  which can be estimated for high and poor quality samples to compare results with changes recorded for the samples DC resistances. Finally, we can decide which of the proposed factors is more effective for detecting differences between the investigated ZnO varistor batches.

Table 2 presents all the proposed factors. We observe differences between the samples of high and poor quality batches greater than hundreds in case of noise measurements and quite tiny variations of DC resistance at the same polarizing current  $I = 200 \mu\text{A}$ . Thus, we can conclude that  $1/f$  noise is a very sensitive tool for ZnO varistor quality evaluation and can be applied for ZnO structures of various dimensions. Similar results were observed when  $S_I(f)$  or  $S_{I_g}(f)$  parameters were considered. Noise data can be applied for determining technology parameters of the produced varistors in

laboratory investigations but due to complicated measurement setup and time of noise recording have very limited application in industrial environment, at presence of high electromagnetic interferences.

## 6. Conclusions

A noise level is a sensitive tool for identification of varistors having different ZnO grain types as a result of sintering in different temperatures. It detects varistors of poor quality and endurance which exhibit much higher  $1/f$  noise intensity than the properly prepared ZnO samples. Variations in grain sizes of ZnO structures suggest variations in their mechanical properties (for example stiffness, sound velocity) which can be also identified by convenient industrial measurements during their fabrication, using ultrasound spectroscopy methods with algorithms necessary for solving inverse problem [5, 29]. Unfortunately, these methods do not differentiate so significantly the samples. The same problem is when the DC resistances at given DC current polarizing varistors are considered. These results were obtained for power spectral density  $S_i(f)$  of  $1/f$  noise measurements only without any assumption about physical parameters used in the Hooge formulae (e.g. assuming value of number  $N$  of free carriers generating noise or estimating number of grains  $N_g$  in the sample volume).

## Acknowledgement

This research was partially supported by the Polish Ministry of Science, project No. 3043/B/T02/2010/38, 2010-2011, the European Centres of Excellence CEITEC CZ.1.05/1.1.00/02.0068, by the project Sensor, Information and Communication Systems CZ.1.05/2.1.00/03.0072 and by the bilateral Czech-Polish research project "Non-destructive testing of electronic material and devices using electro-ultrasonic and resonant ultrasonic spectroscopy" MOBILITY 7AMB13PL033.



## References

- [1] L. K. J. Vandamme, "Noise as a Diagnostic Tool for Quality and Reliability of Electronic Devices", *IEEE Trans. Electr. Dev.* 41 (1994) 2176–2187.
- [2] B. K. Jones, "Electrical noise as a measure of reliability in electronic devices", *Advanced in Electronics and Electron Physics*, 67 (1994) 201–257.
- [3] J. Smulko, "Methods of electrochemical noise analysis for investigation of corrosion processes", *Fluctuation Noise Lett.* 6, (2006) R1–R9.
- [4] L. Hasse, J. Smulko, "Quality assessment of high voltage varistors by third harmonic index", *Metrology and Measurement Systems*, 15 (2008) 23–31.
- [5] L. Hasse, M. Kiwilszo, J. Smulko, T. Stepinski, "Quality assessment of varistor ZnO structures by resonant ultrasound spectroscopy", *Insight*, 51 (2009) 262–265.
- [6] L. Hasse, J. Smulko, M. Olesz, V. Sedláková, J. Šikula, P. Sedlák, "Diagnostics of ZnO varistors by means of nondestructive testing", *Gdańsk University of Technology Faculty of Electrical and Control Engineering Annals*, No. 29, 2011, 59-65.
- [7] L. Hasse, J. Smulko, L. Kaczmarek, "Low-frequency noise in ZnO varistor structures", *Proc. XIX IMEKO World Congress*, Lisbon, 2009, 1354–1358.
- [8] J. Wu, T. Li, T. Qi, Q. Qin, G. Li, B. Zhu, R. Wu, C. Xie, "Influence of dopants on electrical properties of ZnO-V<sub>2</sub>O<sub>5</sub> varistors deduced from AC impedance and variable-temperature dielectric spectroscopy", *J. Electronic Materials*, 41 (2012) p.1970-1977).
- [9] M. Dudek, K. Nitsch, T. Piasecki, A. Dziedzic, "Wide frequency range AC electrical characterization of thick-film microvaristors", *Microelectronics Reliability*, 51 (2011) 1219-1224.
- [10] J. Hoja, G. Lentka: "An analysis of a measurement probe for a high impedance spectroscopy analyzer", *Measurement*, 41 (no. 1 2008) 65-75.
- [11] A. Dziedzic, A. Kolek, "1/f noise in polymer thick-film resistors", *J. Phys. D: Appl. Phys.*, 31 (1998) 2091-2097.
- [12] M.M. Jevtić, I. Mrak, Z. Stanimirović, „Thick-film resistor quality indicator based on noise index measurements”, *Microelectronics Journal* 30 (1999) 1255-1259.
- [13] A.W. Stadler, "Noise properties of thick-film resistors in extended temperature range", *Microelectronics Reliability*, 51 (2011) 1264-70.
- [14] T.K. Gupta, In: *Engineered Materials Handbook*, v. 4, *Ceramics and Glasses*, ASM (1991), p. 1150.
- [15] "ASA – low voltage surge arresters". Catalogue ASA, Apator S.A., 2011.
- [16] E. Olsson, G.L. Dunlop, R. Österlund, "Development of functional microstructure during sintering of ZnO varistor materials", *J. American Ceramic Society*, 76 (1993) 65-71.

- [17] de la Rubia M.A., Peiteado M., de Frutos J., Rubio-Marcos J., Fernandes J.F., Caballero A.C., "Improved non-linear behaviour of ZnO-based varistor thick films prepared by tape casting and screen printing", *J. Eur. Ceram. Soc.*, 27 (2007) 3887-3891.
- [18] Mis E., Dziedzic A., Mielcarek W., "Microvaristors in thick-film and LTCC circuits", *Microelectronics Reliability*, 49 (2009) 607-613).
- [19] F. N. Hooge, "1/f noise is no surface effect", *Phys. Lett. A* 29 (1969) 139–140.
- [20] T. Musha, "Physical background of Hooge's  $\alpha$  for 1/f noise", *Phys. Rev. B* 26, (1982) 1042–1043.
- [21] F. N. Hooge, T. G. M. Kleinpenning, L. K. J. Vandamme, "Experimental studies on 1/f noise", *Rep. Prog. Phys.* 44 (1981) 479–532.
- [22] L.K.J. Vandamme, J.C. Brugman, "Conduction mechanisms in ZnO varistors", *J. Appl. Phys.* 51 (1980) 4240-4244.
- [23] A. Kusy, T. G. M. Kleinpenning, "Conduction mechanisms and 1/f noise in ZnO varistors", *J. App. Phys.*, 54 (1983) 2900–2906.
- [24] M. Prudenziati, A. Masoero, A. M. Rietto, "Conduction mechanisms and flicker noise in ZnO varistors", *J. App. Phys.*, 58 (1985) 345–350.
- [25] H. D. Xiong, W. Wang, J. S. Suehle, C. A. Richter, W. K. Hong, T. Lee, "Noise in ZnO Nanowire Field Effect Transistors", *J. Nanosci. Nanotechnol.* 8 (2008) 1–4.
- [26] A. Kolek, A. W. Stadler, P. Ptak, Z. Zawiślak, K. Mleczko, P. Szałański, D. Žak, "Low-frequency 1/ f noise of RuO<sub>2</sub>-glass thick resistive films", *J. App. Phys.*, 102 (2007) 103718.1–103718.9.
- [27] L. K. J. Vandamme, "Criteria of low-noise thick-film resistors", *Electrocomp. Sci. Technol.* 11 (1977) 171–177.
- [28] L. Yang, J. Gest, G. Leroy, L. K. J. Vandamme, "1/f noise in ZnO films", *21st Int. Conf. on Noise and Fluctuations*, (2011) 90–93.
- [29] J. Mroczka, D. Szczuczynski, "Inverse problems formulated in terms of first-kind Fredholm integral equations in indirect measurements", *Metrology and Measurement Systems*, 16 (2009) 333–357.



## Vitae

Lech Hasse PhD is a Lecturer at the Department of Optoelectronics and Electronic Systems, Gdansk University of Technology, G. Narutowicza 11/12, 80-952 Gdansk, Poland. He is a member of the board of the Polish Society of Theoretical and Applied Electrotechnics in Gdansk, a member of the Instrumentation and Measurement Systems Section of the Metrology Committee of the Polish Academy of Science and a member of the IEEE.

Sylwia Babicz and Leszek Kaczmarek have graduated from the Faculty of Electronics, Telecommunications and Informatics at Gdansk University of Technology, Poland, and now Sylwia Babicz is a Ph.D. student and Lecturer at the Faculty of Electronics, Telecommunications and Informatics, Gdansk University of Technology (ETI, GUT) and Leszek Kaczmarek is a Ph.D. student at ETI, GUT and works in a company in the field of digital signal processing in real-time Systems.

Janusz Smulko PhD DSc is a Professor at the Department of Optoelectronics and Electronic Systems, Gdansk University of Technology, Poland. He is a member of the board of the Polish Society of Theoretical and Applied Electrotechnics in Gdansk, a member of the Microsystems and Sensors Section of the Metrology Committee of the Polish Academy of Science and a member of the IEEE.

Vlasta SedlákováPh.D. is a Docent at the **Faculty of Electrical Engineering and Communication**, Department of Physics, Brno University of Technology, Czech Republic.

## Tables

Table 1. Statistical values of the surface structures of well-prepared specimen (sample no. 100) and poor quality specimen (sample no. 22A).

	well-prepared	poor quality
diameter [ $\mu\text{m}$ ]	1,76	1,57
perimeter [ $\mu\text{m}$ ]	11,94	10,57
size [ $\mu\text{m}^2$ ]	5,52	4,1
volume [ $\mu\text{m}^3$ ]	12,32	9,16

Table 2. Quotients of the current spectral densities  $S_i(f)$  and the estimated by (4) mean spectral density of ZnO grains  $S_{ig}(f)$  at frequency  $f = 100$  Hz for high and poor quality varistor samples (Fig. 10) of different working voltages and thicknesses (280 V, 2.9 mm; 440 V, 4 mm; 660 V, 5.8 mm); DC resistance  $R$  of poor and high quality samples was measured at the same polarizing DC current  $I = 200 \mu\text{A}$  and responding DC voltages presented at Fig. 10.

	$S_{i, \text{poor}}(f)/S_{i, \text{high}}(f)$	$S_{ig, \text{poor}}(f)/S_{ig, \text{high}}(f)$	$R_{\text{poor}}/R_{\text{high}}$
<b>280 V</b>	204	280	1.06
<b>440 V</b>	1690	2360	1.23
<b>660 V</b>	429	601	1.08

## Captions to figures

Fig. 1. Varistor current-voltage characteristics.

Fig. 2. Varistor specimens: a – ZnO structures after being fired (top row) and with a metalized contacts (bottom row); left – 280 type, middle – 440 type, right – 660 type; b – surge arrester produced by Aparator S.A. [15] with ZnO-based varistor.

Fig. 3. Scans of ZnO surface of exemplary varistors prepared for working at 280 V and taken by Atomic Force Microscope: a) well-prepared specimen with large grains (sample no. 100), b) poor quality specimen with smaller grains (sample no. 22A).

Fig. 4. Fig. X The topography of ZnO surface after Laplace filtering with marked examples of grains of a) well-prepared specimen (sample no. 100), b) poor quality specimen (sample no. 22A).

Fig. 5. Histogram of ZnO points height distribution estimated by surface scanning of exemplary varistors prepared for working at 280 V and taken by Atomic Force Microscope (Fig. 3): a) well-prepared specimen with large grains (sample no. 100), b) poor quality specimen with smaller grains (sample no. 22A).

Fig. 6. Current-voltage characteristics of typical varistor specimen: poor (red squares) and high (blue circles) quality; the tested samples were designed for working at 280 V.

Fig. 7. General block diagram of noise measurement system.

Fig. 8. High-voltage set-up with current-voltage converter by using OPA128 operational amplifier.

Fig. 9. Power spectral density  $S_I(f)$  of current fluctuations across the tested varistors (280 type), nos. 45, 60, 63; the DC current across the specimen was  $I = 11 \mu\text{A}$ , the measurement frequency interval was up to 6.4 kHz.

Fig. 10. Current power spectral density  $S_I(f)$  of exemplary varistors of 280 type: a) versus their bias DC current  $I$  at frequency  $f = 2 \text{ kHz}$  and b) their corresponding DC current-voltage characteristics.

Fig. 11. Power spectral density  $S_I(f)$  of current fluctuations versus frequency  $f$  for varistor samples of high quality (nos. 91, 124, 60) and poor quality (nos. 98, 26, 96); the samples were: a) 280 type(nos. 91, 98), b) 440 type(nos. 26, 124), c) 660 type(nos. 60, 96); the attached (d) ÷ f), respectively) important parts of their I-V characteristics show functional differences for high and poor quality samples.

## Figures

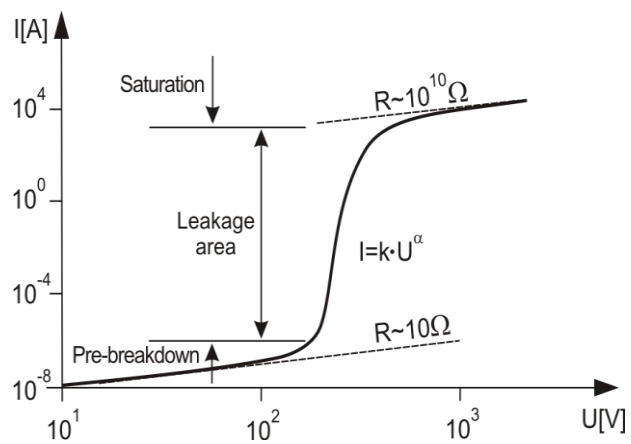


Figure 1



Figure 2

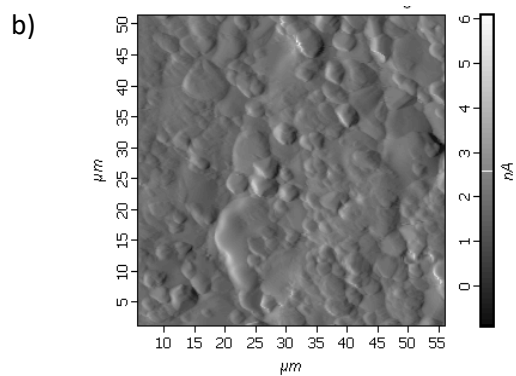
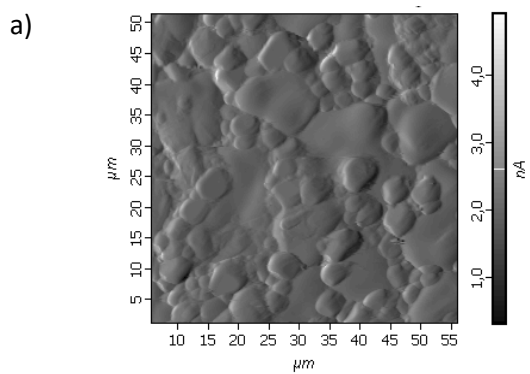
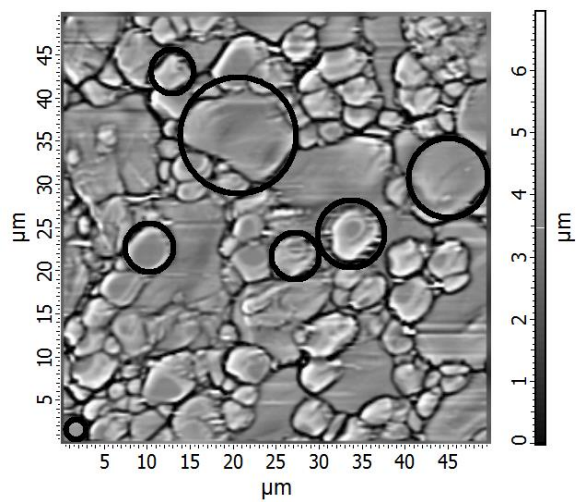


Figure 3

a)



b)

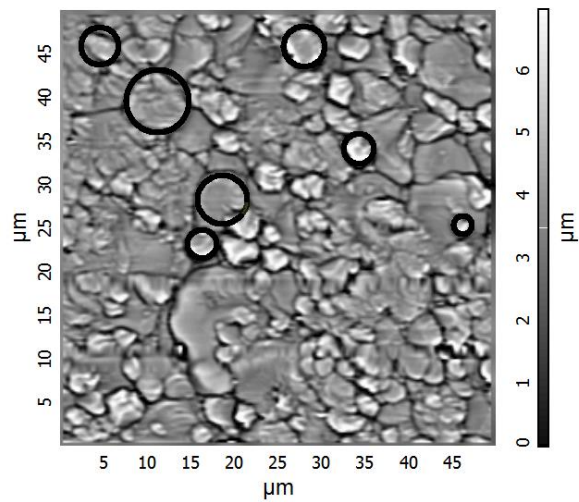
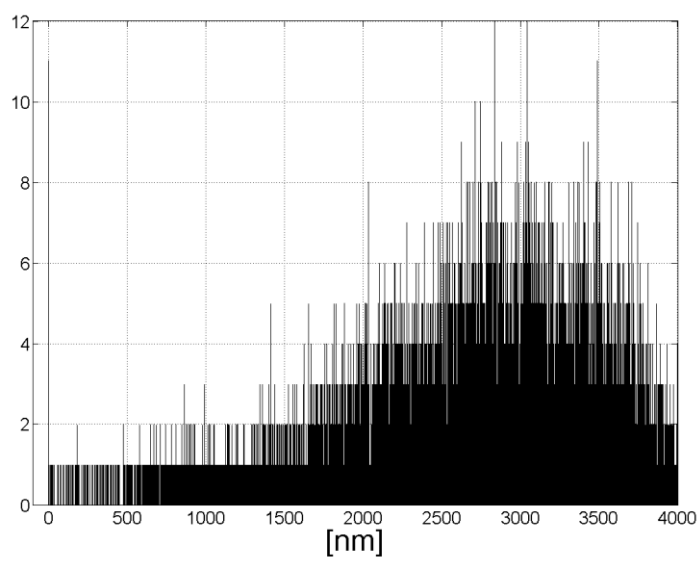


Figure 4

a)





b)

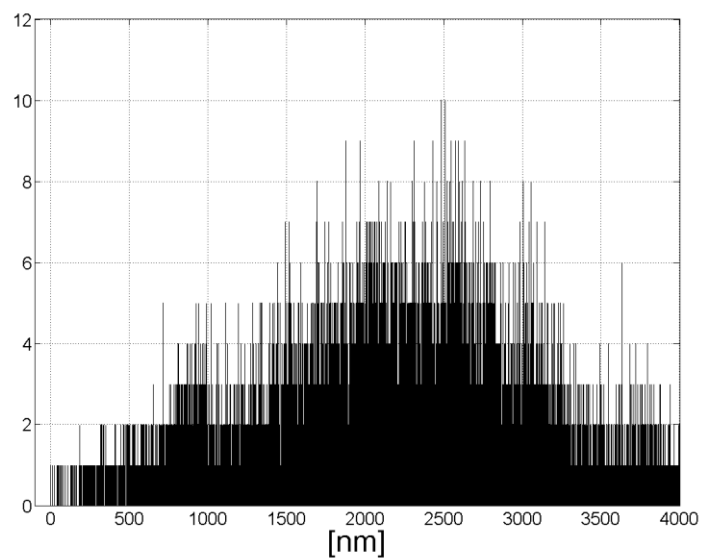


Figure 5

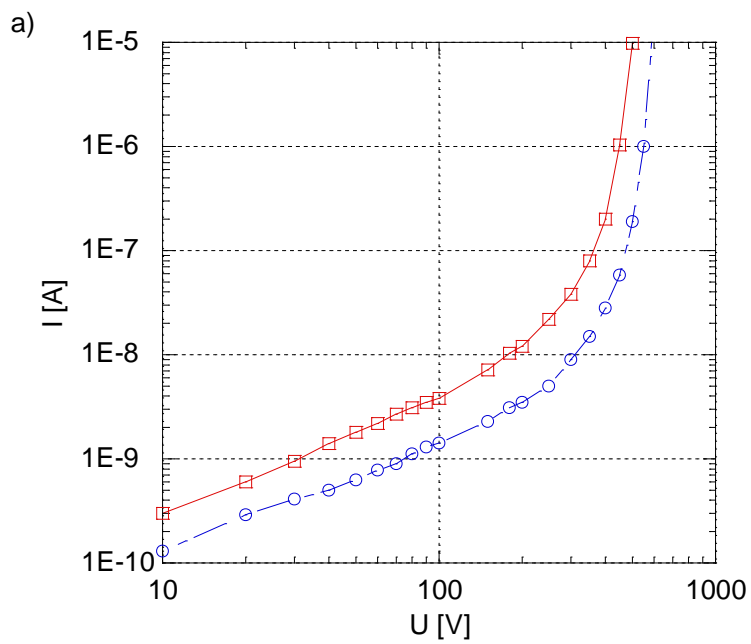


Figure 6

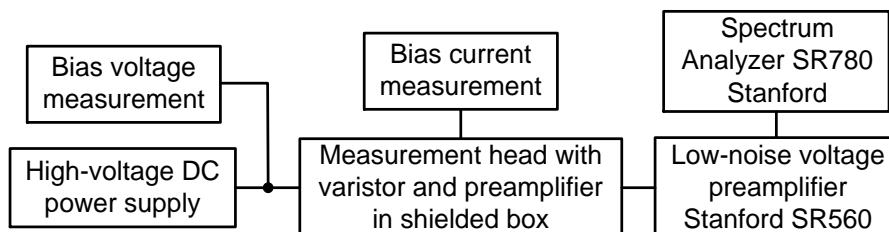


Figure 7

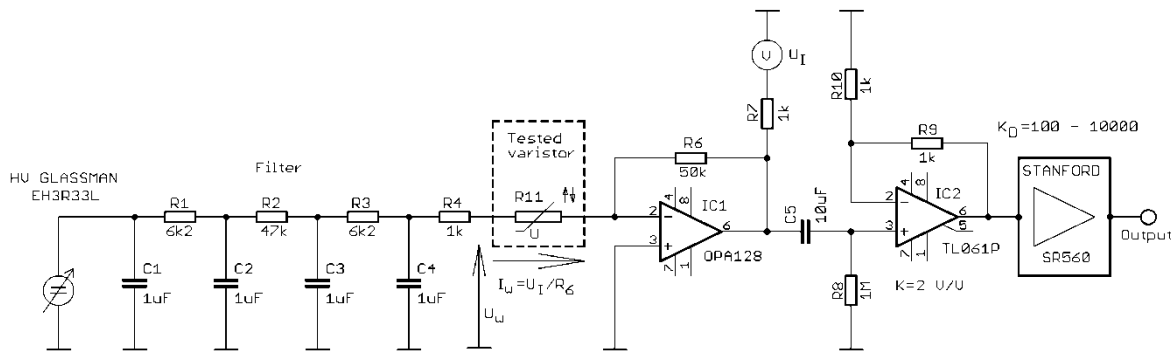


Figure 8

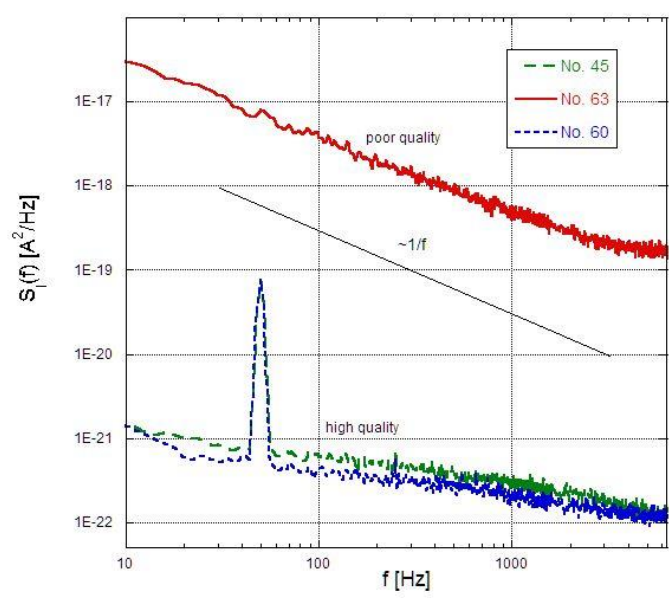
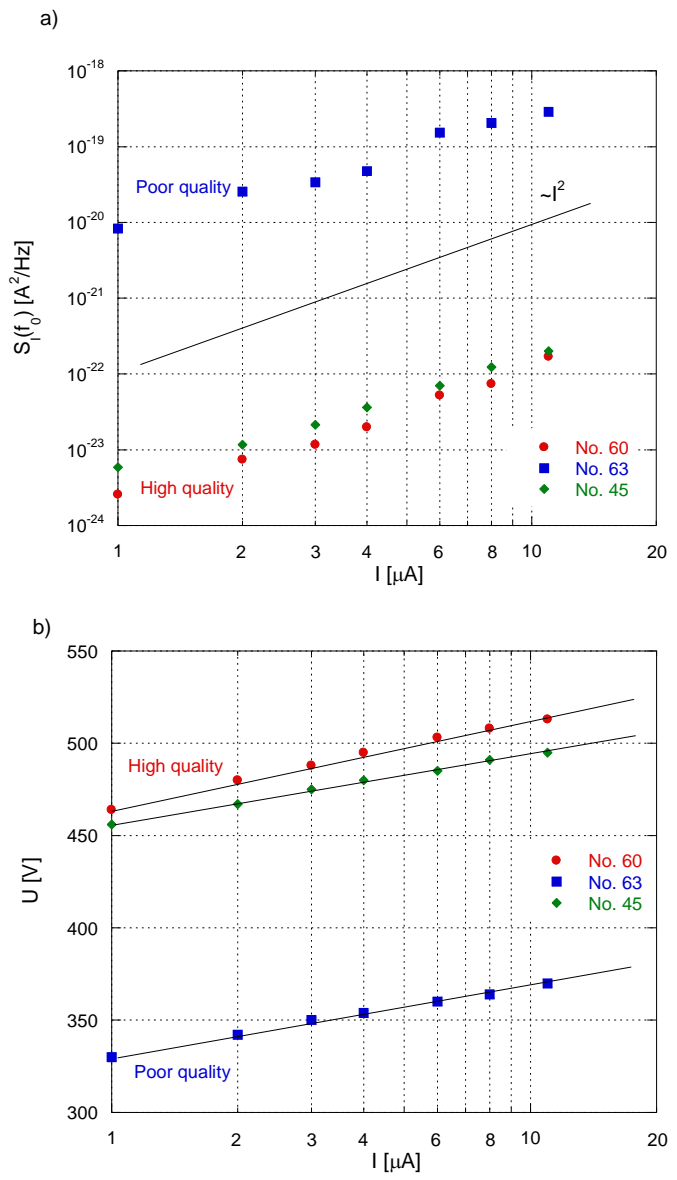


Figure 9



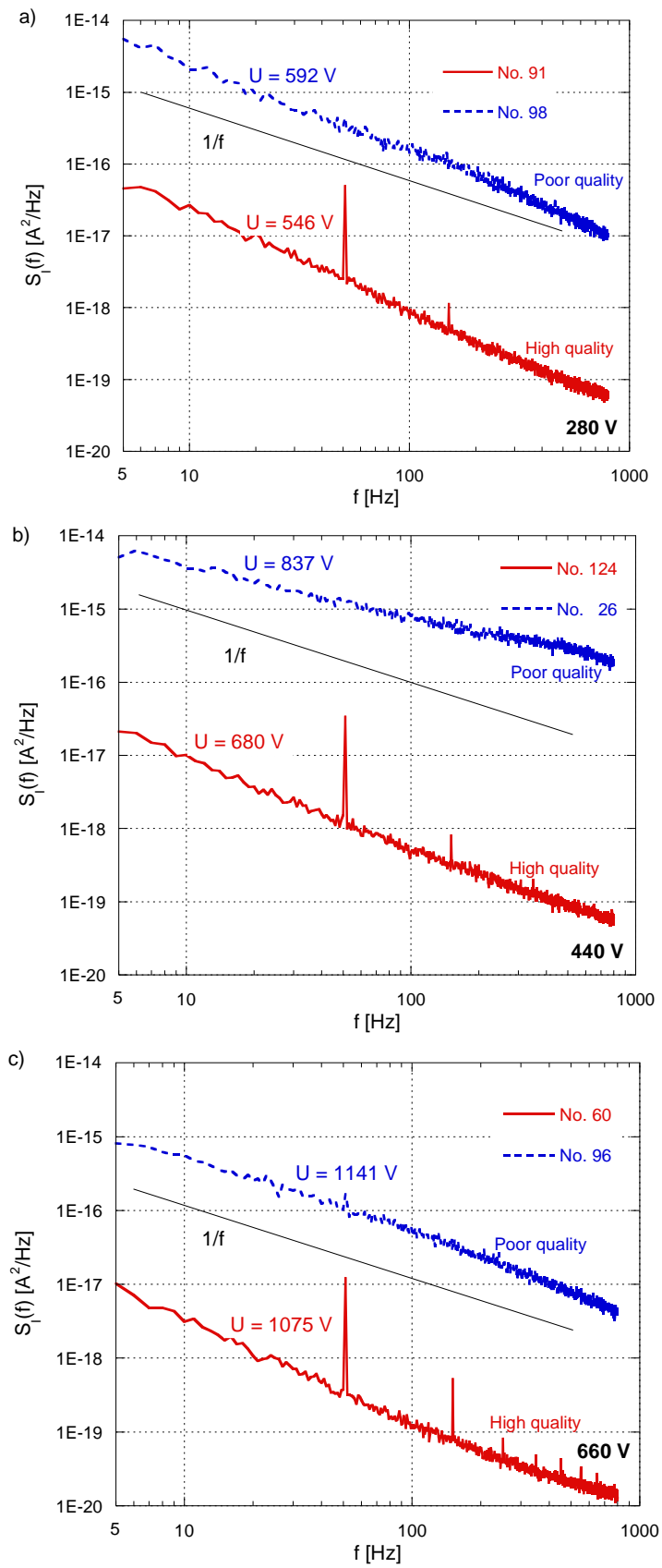


Figure 11